Electron Diffraction and Surface Structure.

OPENING CONTRIBUTION TO A DISCUSSION HELD JOINTLY WITH THE PHYSICAL SOCIETY ON MARCH 17TH, 1938.

By G. I. FINCH.

THE chemical and physical properties of a solid depend not only upon chemical composition but also upon the way in which the atoms and molecules are arranged. Owing to high penetrating power, *X*-rays reveal only internal structure; we cannot, however, argue from a knowledge of the internal structure of a solid to that of its surface. But the chemistry and physics of the solid state depend largely on the properties of the gas–solid and the liquid–solid interfaces. Thus it is not surprising that, failing any direct method of study, chemical and physical properties, not necessarily of the surface alone but sometimes also of the mass, and determined by an almost bewildering variety of methods and supplemented by *X*-ray information as to the underlying atomic structure, have had in the past to serve as the basis for deducing the nature of surface structure.

Apart from chemical examination, the more usual methods of surface study have depended upon the phenomena of the scattering of light, generally of a wave-length well within the visible range and from which the eye or the microscope can build up an image; or interference effects are observed in the scattered radiation. The microscope shows the topography of the surface from objects of any size or order in shape or arrangement down to details whose dimensions are of the order of that of the wave-length; whilst interference (diffraction) phenomena can only disclose the existence of regular features whose linear dimensions are of the order of the wave-length. Thus the detail of atomic arrangement in structure is far beyond the powers of resolution of these methods which can only serve to enable us to infer, in favourable cases, the nature of such structure.

The experimental proof of the wave properties of moving electrons not only settled a conflict which had dominated physics for many years but also put into our hands a powerful tool for the study of the atomic structure of surfaces, the potentialities of which it would be hard to exaggerate in view of the importance of the new fields now open for the first time to direct study. Unlike *X*-rays, electron waves are associated with an electrostatic charge; thus it is the nucleus with its intense field rather than the surrounding screen of orbital electrons which plays the chief rôle in the scattering of moving electrons. Herein lies the reason for the great efficiency of the scattering of electrons by atoms, roughly a million times that of *X*-rays. It follows that, whilst with *X*-rays the surface scattering is so slight as to be wholly swamped by that due to the bulk of the underlying material, the depth to which electrons can penetrate coherently into matter is confined to a few atomic layers at the surface. Thus the information which the scattering of electron waves can give is confined to these surface layers. The wave-length associated with electrons of the speeds normally used in structure analysis is of the order of 0·05 A., but the difficulties of electrostatic and electromagnetic lens design are such that the potential resolving power of the electron microscope is far from having been realised; in electron diffraction, however, where the technique is almost as simple as that of *X*-rays, this has to all intents and purposes been attained.

The early experiments on the wave properties of moving electrons disclosed points of similarity between the phenomena of the diffraction of *X*-rays and electron waves, but it soon became evident that in many other respects the parallel could not be drawn. The

value of the electron-diffraction method of structure analysis must depend, however, on a proper appreciation of the significance of the associated phenomena. This accounts for the fact that, in addition to improving the experimental technique, attention has been mainly directed towards building up the interpretative technique rather than to the systematic study of specific surface problems. Nevertheless, electron diffraction has already added so much to our knowledge of surface structure that, instead of trying to summarise such contributions, my present aim must be to illustrate its potentialities by means of a few examples without going specially into the question of interpretation, a subject which has been fully dealt with in several recent monographs.

In electron diffraction, the angles of deviation and the relative intensities of the rays diffracted by the atoms of a surface film are recorded photographically in a plane normal to the electron beam at a known distance from the specimen. When the layer can be detached and examined in the form of a film thin enough to transmit the electron beam without excessive inelastic scattering, the whole pattern surrounding the point of impact of the main electron beam can be recorded as, for example, in Fig. 15, the plane of the film being normal, or more or less steeply inclined, to the beam. Otherwise, the layer must be examined with the beam grazing the surface, in which case the massive substrate casts a shadow which obscures rather more than half the field, as in Fig. 3. The electron-diffraction pattern is a record from which it should be possible to read the nature of any regularity in the average atomic arrangement in the surface layer. The amount of information we may wish to extract from the pattern, however, depends upon the nature of the problem.

The chief feature of regularity in a monatomic liquid, such as a molten metal, is the nearest distance of approach of the atoms, *i.e.*, the atomic size. The corresponding *X*-ray pattern reflects this low degree of order of atomic arrangement in that it consists of a few diffuse haloes more or less submerged in a background of general scattering. Hence, when Thomson and French and Raether obtained electron-diffraction patterns of this type (Fig. 1) from mechanically worked, *i.e.*, polished, burnished, or hammered metallic surfaces, they regarded this as evidence of the amorphous state of the polish layer which Beilby had conclusively shown to be formed by a smearing over the surface of metal caused to flow by the polishing action. This view was challenged by Kirchner, who found that some metal surfaces which were certainly crystalline also gave rise to halo patterns, possibly because their extreme smoothness limited the access of the electron beam to exceedingly small portions of the individual crystals. The discovery by electron diffraction, however, that the metallic polish layer possessed the liquid-like property, not shared by the metal in the crystalline state, of dissolving at room temperature crystals of another metal (Fig. 2), strongly supported the view of the amorphous nature of the polish layer and of its formation from material caused to flow in the liquid state and then frozen with such abruptness on cessation of the polishing action as to allow insufficient time for the atoms to re-arrange themselves regularly on solidification. Bowden and Ridler furnished convincing evidence of the occurrence of such liquid flow during polishing when, by making use of the thermo-electric property of pairs of different metals, they showed that the temperature of burnishing, *i.e.*, polishing, was limited to that of the melting point of the more readily fusible metal. Further, Cochrane has recently succeeded in detaching a gold polish layer from its substrate and found that it yields by transmission a halo pattern which gradually in time develops into one of well-defined rings; thus showing that, whilst a freshly detached polish layer is at first amorphous, it tends slowly to recrystallise. Thus, in the light of all this evidence, and seeing also that the metallic polish layer differs both physically and chemically from the crystalline surface in that it is, for example, both harder and more readily etched, it seemed justified to regard the electron-diffraction halo pattern obtained from a worked metallic surface as characteristic of an amorphous structure.

Beilby had found that the phenomenon of surface flow occurs not only on metals but also on non-metallic substances and is, indeed, strikingly easy to demonstrate on calcite. This led him to infer that the polish layer is amorphous not only on metals but also on non-metals and, in particular, on a cleavage face of a single crystal of calcite. In this Beilby was mistaken, for Raether and Hopkins obtained from polished calcite single-crystal

cleavage surfaces patterns of such a nature as to establish clearly that the polish layer was of single-crystal structure integral with that of the underlying calcite crystal (Figs. 3 and 4). Nevertheless, there is no doubt that in this case polishing produces a surface flow which leads to the building up of a layer of several thousand Ångströms in depth, as Beilby was able to show. Thus it seems that the flowing material cools sufficiently slowly on a calcite cleavage face for the molecules to be able to order themselves under the influence of the atomic forces at the interface between the crystal substrate and flowed layer.

There is no apparent reason to suppose that the crystallographic nature of the polished face can have much effect on the rate of cooling of the flowed layer; on the other hand, the atomic forces at the crystal-polish interface must be a function of the nature of the atoms and of their density and mode of packing. Hence, the ability of the crystal face to order the calcite molecules of the flowed layer into line with the substrate structure should depend upon its crystallographic nature. These forces should be much weaker in a calcite crystal surface steeply inclined to all possible cleavage directions than in a cleavage plane. Experiment proves this to be the case, for the polish layer on a calcite crystal face so inclined yields a halo pattern characteristic of the amorphous state. Sufficiently prolonged heating of the surface, however, even to far below the melting point, confers enough mobility upon the disordered molecules to enable the interfacial atomic forces to line them up into a structure continuous with the substrate crystal (Fig. 5).

It so happened that Beilby became familiar with a phenomenon which might well have led him to infer correctly the structure of polish on calcite, had he not by that time been convinced that the occurrence of surface flow necessarily established the amorphous nature of polish. Beilby found that crystals of sodium nitrate, the structure of which is isomorphous with that of calcite, when grown from a film of the solution on either a fresh or a polished cleavage face of calcite were so orientated as to continue as closely as possible the structure of the calcite (Fig. 6). He interpreted this as evidence of a remarkable range of the atomic forces at the polish-layer–crystal interface, in that they were apparently able to control the orientation of the nitrate crystals even through the several thousand Ångström thick polish layer which he supposed to be amorphous. Intense though such forces may be at ranges of atomic dimensions, however, they must fall off in accordance with an inverse sixth-power law to become wholly negligible at far less distances than the thickness of the flowed layer. Had this occurred to Beilby, he would no doubt have inferred from the orientation of sodium nitrate on a polished calcite cleavage face that in this case the polish layer was of single-crystal structure integral with the main crystal, and would generally have reached conclusions similar to those to which we have been led by electron diffraction. The validity of such conclusions drawn from crystal overgrowth experiments is shown by the fact that sodium nitrate does not orientate (Fig. 7) on the polish layer on a calcite surface steeply inclined to all cleavage directions and which electron diffraction has shown to be amorphous, but does so readily (Fig. 8) once the surface has been caused by heating to recrystallise and thus yield a pattern (Fig. 5) typical of a single-crystal structure.

Unlike the metals, the polish layer on which has so far always proved to be amorphous provided reasonable precautions have been taken to prevent oxidation or the occlusion of grains of the polishing material, the non-metals may be divided into four classes, according to the nature of the surface changes effected by polishing as shown by electron diffraction. Surface flow does not occur on the diamond or on graphite, which thus fall into a class by themselves in that they provide the only examples known where polishing simply levels the surface—in the case of the diamond by wearing down protuberances (Fig. 9), and in that of graphite by causing the crystals to orientate and slip with their cleavage planes in the directions of the applied shear stresses (Fig. 10). In another class, containing for example kyanite and calcite, the structure of the polish layer may be either crystalline or amorphous according to the crystallographic nature of the surface. Of the remaining two classes, one consists of minerals such as quartz (Fig. 11), garnet, and corundum where the polish layer is crystalline, whilst the other comprises zircon, cassiterite, the spinels (Figs. 12 and 13) and others which form amorphous polish layers irrespective of the crystallographic directions of the surface.

The fact that the polish layer on corundum is crystalline whilst that on spinel, a solid solution of magnesium oxide in alumina, is amorphous is of some practical interest in that it bears upon the question of wear in the high-speed internal-combustion engine, part of which can be attributed to the oxide coating on the aluminium piston. This coating gives a halo pattern and is thus amorphous, but the polishing action of running-in converts it into a polycrystalline film of γ-aluminium oxide and corundum (Fig. 14) on which the surface-flowed material always recrystallises and thus produces a hard surface which, in terms of atomic dimensions, is relatively rough. But the oxide coating on an aluminium piston, the surface layer of which is alloyed with magnesium, gives a spinel when subjected to friction and acquires a permanently amorphous and therefore smooth polish layer.

The amorphous structure of the oxide on aluminium surfaces was first demonstrated by Preston and Bircumshaw, who vaporised aluminium foil in a stream of dry hydrogen chloride and so isolated the thin oxide film to which aluminium owes its relatively high resistance to corrosion. Electron diffraction showed that this oxide film is amorphous. At about 700°, however, at which temperature also aluminium begins to oxidise relatively rapidly, the amorphous oxide crystallises, forming a polycrystalline film through the many comparatively large interstices of which oxygen can enter and attack the metal. Transmission patterns from a thin single crystal of aluminium, an edge of which has been heated in a Bunsen flame, show these features remarkably well. As the electron beam is moved from the unheated part of the specimen towards the heated area, the pattern changes from one of diffraction spots, due to the aluminium crystal, and diffuse haloes, due to the amorphous oxide, to sharp rings characteristic of unorientated γ-aluminium oxide crystals; and at an intermediate position it is possible to secure a pattern (Fig. 15) exhibiting all these features simultaneously.

Another example of immunity to oxidation conferred by an amorphous layer is that afforded by the silica film with which silicon carbide is coated as a result of superficial oxidation during cooling of the charge in the process of manufacture. This silica skin can easily be removed by, for example, abrasion with a material harder than silica but too soft to affect the carbide. A crystal prepared in this manner gives a brilliant single-crystal pattern typical of the carbide structure (Fig. 16); but it can be heated in air even to white heat or in an oxygen–coal-gas flame without inducing rapid combustion. Electron diffraction shows that such treatment causes the formation of a fresh thin skin of amorphous silica, the rate of growth of which in relation to the temperature of heating affords a measure of the protection it gives to the carbide against oxidation. Thus the film formed on a clean carbide crystal heated to a bright red heat in an oxidising atmosphere is, even after two minutes, still so thin that the electron beam at grazing incidence can penetrate to the unchanged carbide crystal surface and give its characteristic pattern, though partially obscured, it is true, by the pattern of haloes and general background scattering due to the amorphous silica (Fig. 17). A calculation due to Thomson suggests that if the amorphous film were of gold it would need to be only about 15 A. thick in order to suppress coherent scattering from the carbide surface. In view of the smaller atomic numbers of silicon and oxygen, however, this is probably an under-estimate. We can, however, obtain directly a good idea of the depth of penetration of the electron beam at grazing incidence as follows. A unimolecular layer of a normal straight-chain hydrocarbon on a plane surface gives a reflection pattern (Fig. 19) of parallel lines showing that the molecules are standing erect on the surface. By forming, then, unimolecular pure paraffin layers of different chain lengths on a smooth single-crystal surface, we can find out that chain length necessary to obscure all signs of the single-crystal pattern. Thus a $C_{22}H_{46}$ layer on a smooth quartz crystal face gives a composite hydrocarbon–quartz crystal pattern (Fig 18); with $C_{28}H_{58}$ the quartz pattern is feeble, and with $C_{32}H_{66}$ entirely absent (Fig. 19). Hence the upper limit of penetration of the electron beam at grazing incidence is less than 43 A., the length of the $C_{32}H_{66}$ chain. The thickness of the protective coating of amorphous silica formed on silicon carbide after two minutes' heating to a bright red heat is therefore much less than 43 A.

The resistance to corrosion exhibited by many metals is due to the formation of a protective film, frequently an oxide. Although work in this field is only beginning, the

general rule so far emerges that the smaller the crystal size of the film, the greater the degree of protection it confers. For instance, the oxide film (α-ferric oxide) formed by heating iron in air consists of relatively large crystals of the rhombohedral system (Fig. 20) and gives little protection. Films obtained by some of the commercial blueing processes have much smaller crystals of cubic system and consisting of γ-Fe_2O_3 or Fe_3O_4 (Fig. 21); but although affording fair protection against atmospheric corrosion, they are not nearly so effective as the practically amorphous skin formed by the nitric acid (Fig. 22) or potassium chromate passivation of iron. When heated in a vacuum to 650°, this amorphous skin crystallises to γ-Fe_2O_3 or Fe_3O_4 (Fig. 23) and loses its protective qualities. Thus, as in the case of the oxide films on aluminium and silicon carbide, protection seems to be largely a question of film continuity. When a crystalline oxide is formed on a metal surface, the crystals are usually orientated in such a way that the oxide crystal plane most rich in metal atoms is in contact with the metal surface, irrespective of whether this be amorphous, polycrystalline, or of single-crystal structure. Owing to the change in lattice dimensions, the individual oxide crystals cannot fit closely together, but an amorphous oxide may well be continuous in the sense that it is free from interstices large enough to permit of the passage of oxygen, because the intermolecular distances are not so rigidly fixed as in the crystalline state.

A crystalline oxide film formed by blueing iron or by heating an amorphous iron oxide layer was mentioned above as consisting of γ-Fe_2O_3 or Fe_3O_4. Since no two chemical compounds can have exactly the same structure, it might be thought that the beautifully clear patterns (Figs. 21 and 23) furnished by this film would enable us to identify the precise nature of the oxide. This, however, is one of those rare cases where the crystalline structures of two compounds are so much alike that their ring patterns are difficult to distinguish the one from the other. In nearly all cases, however, electron diffraction is proving to be by far the surest if not indeed the only method of identifying the nature of thin surface films formed by chemical attack. In solving such problems, the nature of the original surface and the conditions of attack are generally known. It is also useful, though by no means indispensable, that the crystal structures of most of the compounds likely to enter into the composition of the film have been determined by *X*-rays. A few examples will suffice to illustrate this. Thomson obtained two distinct, different crystalline films by heating copper in air. One of these was certainly cuprous oxide, since its pattern (Fig. 24) showed that it had both the structure and the lattice dimensions agreeing with those previously assigned to this compound by *X*-rays. The other oxide film had a more complicated structure, quite different from that then attributed by *X*-rays to cupric oxide. Hence, if the *X*-ray data were correct, and there seemed to be no reason to doubt this, it followed that the film in question could not be cupric oxide but must be a new, unknown oxide of copper. Later, however, by comparing its diffraction pattern (Fig. 25) with that obtained from tenorite, the oxide was identified as cupric oxide, a conclusion which was confirmed when a fresh analysis by *X*-rays revealed the fact that the structure of cupric oxide was monoclinic and not triclinic as had hitherto been supposed.

The film formed on nickel heated in selenium vapour gives a pattern (Fig. 26) which is identical, except for a slight difference in ring radii, with that obtained from pyrites. Thus its composition is $NiSe_2$, the difference between its lattice dimensions and those of ferric sulphide being due to the different sizes of the respective atoms. In this case, not only was the structure unknown to *X*-rays, but the compound itself was previously supposed to have the composition NiSe. As other examples I would cite the case of a white bloom formed on a silver catalyst surface and thought to be an oxide, but immediately identified by electron diffraction as metallic silver; and an invisible film resulting from the attack of a hot polished copper surface by trichloroethylene vapour and which proved to be cuprous chloride. Indeed, many other cases could be quoted where the conditions are such that microanalysis or, for that matter, any other method of examination fails, but where electron diffraction can so easily and certainly furnish an answer.

We have seen that the orientation which the crystals formed by chemical attack of a polycrystalline solid surface tend to take up is usually unrelated to that of the substrate crystals, but is generally such that in the compound a metal-rich crystal plane is parallel

to the surface. On amorphous and especially on liquid surfaces the orientation is even more sharply pronounced, no doubt owing to the smoothness of the substrate. For instance, Jenkins found that the crystals of the oxide films, or rather scums, formed on the surfaces of molten liquids were strongly orientated in this way, and mercuric halide crystals grow on a mercury surface in like manner (Fig. 27). The fact that the more densely packed the atoms are in a crystal plane, the more rapidly does the corresponding face grow in area, seems to afford a reasonable explanation for the closely packed type of plane being in contact with the surface. Much the same thing occurs when a film is formed not by chemical attack but by deposition or condensation on an amorphous surface where the atomic forces are not ordered in any particular way. For example, when sodium nitrate crystals are grown on a glass surface or on an amorphous calcite polish layer, they grow as rhombs with one face in contact with the surface, but are otherwise unorientated (Fig. 7). Similarly, in films formed from a vapour stream impinging normally on to an amorphous surface, the crystals tend to take up an orientation such that the most densely packed plane is parallel to the surface, especially if the substrate is heated so that migration of condensed atoms over the surface is facilitated. Burgers and Beeching, however, have shown that if the vapour stream from which the crystals are grown arrives obliquely at a cool surface, then the orientation is more usually such that the plane of densest atomic packing is, as we might expect, normal to the direction of the stream. When the substance is crystalline, however, the orientating effect of the atomic forces at its surface may become the preponderating factor in determining the orientation in films deposited thereon. Thus we have already seen that a crystalline calcite face causes sodium nitrate overgrowth crystals to orientate in such a manner as virtually to continue the calcite structure (Figs. 6 and 8). Generally speaking, however, such an effect calls for the existence of some close relationship between the substrate and deposit crystal structures. In this field there is room for much more work, but it does seem as if equality in the angles between important atom rows rather than a similarity in lattice dimensions were the governing influence. For example, almost perfectly orientated single-crystal films of silver and of other face-centred cubic metals can be grown on both rock-salt and potassium bromide cleavage faces (Fig. 28), although the corresponding lattice constants are 5·63 and 6·58 A. respectively as compared with 4·08 A. for silver. In some cases, however, the deposit crystals will take up an orientation differing from that of the substrate but nevertheless definitely related to its structure. For instance, when iron is electrodeposited on a cube face of gold or on palladium (Fig. 29) the crystals grow with a cube face in contact with a similar face of the basis metal, but the respective cube edges are slewed round through 45° to each other. As a result, the two lattices can fit together practically perfectly in a way which thus represents the most strain-free arrangement at the interface and so guarantees the strongest possible adhesion between the two structures. It seems to be a general rule that, when the electro-deposition conditions are such that the deposit crystal orientation is not controlled, at least in the initial stages, by that of the basis metal, the adhesion of the deposit is poor. Thus a nickel electrodeposit tends to follow the orientation of a copper substrate, but if the deposition be arrested for a short time it often happens that the subsequently deposited nickel fails to continue the orientation, and in such cases the film thus formed can easily be stripped off.

The microscope is often used to infer the continuation of orientation and crystal size in electro-deposits. When we consider the remarkable change in orientation when iron is electrodeposited on gold or palladium, it will be obvious that inferences based on micro-scopic evidence as to the relation between the orientation of deposit and substrate must be of dubious value, and even in regard to crystal size the microscope can give an erroneous impression, especially in the case of metals prone to form deposits of submicroscopic crystal size. For example, nickel deposited under suitable conditions on copper will at first form crystals similar in orientation and size to those of the substrate (Fig. 30), but with increasing deposit thickness the crystal size decreases until the grains can no longer be resolved in the microscope, and the crystal orientation changes completely to one characteristic of the deposition conditions (Fig. 31). Surface examination by the micro-scope fails to note the change and, indeed, gives the false impression that both crystal

size and orientation are continued throughout the deposit (Figs. 32 and 33). Homès has observed a similar phenomenon in the case of an iron surface, the crystals of which had been broken up by cold bending. Subsequent annealing in a vacuum left the surface appearance unchanged even after etching to a depth of nearly a millimetre; *X*-rays, however, showed what the microscope failed to reveal, namely, that the surface crystals had during annealing all grown into and formed part of a single crystal which carried on its surface, and to a considerable depth below, the markings of the original crystal boundaries formed by cold-working. In such cases microscopic examination would probably be more useful, though still not necessarily certain, if the surfaces were viewed in polarised light with the object of throwing the reflexes into greater relief.

An alloying between substrate and electrodeposit has not so far been clearly established. Nevertheless, the change in lattice constants from basis metal to deposit seems to show a tendency to be a gradual one. Thus, Cochrane found that nickel and cobalt electrodeposits on copper have, at and near the interface, lattice constants equal to those of the copper. This seems to be another example of the remarkable pseudomorphism observed when aluminium was deposited from the vapour to form a thin film on platinum. The length of the side of the crystal unit cube of platinum is 3·91 A., and that of aluminium normally 4·04 A. In this case, however, the pattern (Fig. 34) shows that the aluminium deposit crystals were tetragonal with a base in contact with the platinum of 3·91 A. and a height of 4·04 A., showing that the aluminium atoms adjacent to the platinum were compressed together to fit the platinum lattice, but were otherwise free from this constraint and could take up their normal distances apart.

Unlike electrodeposition, chemical displacement of one metal by another leads to alloying, as is shown by chemical analysis. The structure of the alloys thus formed resembles that of the parent metals, from which it is chiefly distinguished by the difference in lattice constants. For example, a platinum film partly displaced by silver and treated with ammonia followed by nitric acid continued to yield a pattern (Fig. 35) characteristic of a face-centred cubic structure but with lattice dimensions intermediate between those of platinum and silver.

We have seen previously how paraffins of known chain length can serve as sounding rods to plumb the depths to which an electron beam can penetrate coherently. Thus the fact that the layer-lines in the reflection pattern (Fig. 19) from a unimolecular film of $C_{32}H_{66}$ deposited on a quartz crystal surface or, for that matter, on any smooth surface, metallic or otherwise, do not change when the surface is rotated in its own plane shows that the hydrocarbon chains must be standing vertically erect on the surface. But the pattern tells much more than this. Since the layer lines are parallel to the shadow edge of the pattern the carbon atoms which act as the main scattering centres must lie in straight rows normal to the surface, and the distance apart of these lines corresponds to a C–C spacing of 2·54 A. in such a row. The breadth of the layer lines relative to their distance apart suggests a row length of about 16 carbon atoms, so there are two such parallel rows in each $C_{32}H_{66}$ molecule. The intensity distribution in the layer lines shows that in the molecule these rows are about 0·9 A. apart, and that in the unimolecular layer the carbon atoms must lie in planes parallel to the surface at 1·27 A. apart, *i.e.*, at half the C–C spacing in the rows. Hence it may be concluded that the carbon atoms in each paraffin chain lie in a plane containing the molecule axis and are situated at the corners of a zig-zag of tetrahedral angle, the alternate C–C spacing being 2·54 A. The intensity distribution suggests further that the molecules are symmetrically packed together in groups, the unit of structure of the molecule packing being a rectangle of about $5 \times 7{\cdot}4$ A. with one molecule erect at each corner and another, also erect, at the centre of the rectangle. An approximately unimolecular layer supported on a thin celluloid film gives the transmission patterns Fig. 36 or 37 when normal to or inclined towards the beam; these not only confirm the value of 2·54 A. for the alternate C–C spacing, but also afford a more accurate measure of the dimensions of the rectangular packing unit, whose sides are now found to be 4·96 and 7·42 A. It is true that similar conclusions have also been drawn from *X*-ray studies of paraffin crystals combined with surface-tension data furnished by the Adam–Langmuir tank technique; but one cannot help being struck by the way in which electron diffraction has

given us this wealth of information directly and in the compass of three easily obtained diffraction patterns.

If, instead of a normal paraffin, a substituted straight-chain compound, *e.g.*, stearic acid, be used to prepare a film by evaporation of a solution on a smooth, plane, stainless-steel surface, we obtain, instead of horizontal layer lines, a pattern of diffuse layer-line envelopes (Fig. 38). These do not change on rotation of the surface in its own plane, and their radii correspond approximately to 2·54 A., *i.e.*, to the alternate C–C spacing in the chains. This shows that in the case of an end-substituted normal paraffin the long chains are no longer erect on the surface but tilted over, to some definite angle, in this case about 53° to the surface, but are otherwise pointing in all possible directions. The inclination of the molecules to the surface can be quantitatively explained on the assumption that strong lateral forces attract and bind the chains together like fascines to a density characteristic of the packing of normal long-chain paraffins. Where the end group in a substituted compound, however, occupies more space than the methyl group, this density of sideways packing is only possible when the chains lean sufficiently far over towards the surface, the degree of tilt from the normal increasing with the effective size of the end group.

A striking and simple experiment, the results of which can only be appreciated directly by electron diffraction, consists in rubbing such a stearic acid layer: if a plane metallic surface on which has been deposited a stearic acid layer be firmly rubbed with filter-paper in one direction, it gives the pattern shown in Fig. 39 when the electron beam grazes the surface in the direction of rubbing. The diffuse arcs of Fig. 38 have now been replaced by a pattern of well-defined features symmetrically disposed about the plane of incidence of the electron beam. It follows that all the molecules, which prior to rubbing had been unorientated in the sense that though inclined by 53° to the surface they were otherwise distributed at random, now point in a direction lying in the plane of incidence which also contains the direction of rubbing. On rotating the surface in its plane, the pattern symmetry decreases until, at 90° to the previous position and therefore with the beam normal to the direction of rubbing, a pattern (Fig. 40) is obtained which exhibits a maximum degree of asymmetry with respect to the plane of incidence, and reveals the fact that the chains are now all inclined at about 5° to the surface and towards the direction of rubbing. A single firm stroke in the opposite direction suffices to re-orientate the molecules towards that direction, and if the surface be rubbed in all manner of ways it is the direction of the last stroke only which determines the final orientation of the stearic acid chains. Figs. 39 and 40 show that, although the acid chains are inclined by 5° to the surface, they are still packed together like the normal paraffin molecules in the sense that, in a plane normal to the molecule axis, the packing unit is still a rectangle of about $5 \times 7{\cdot}4$ A.

A shear stress applied parallel to a paraffin unimolecular film should cause the molecules to incline, the effect increasing with chain length. Hardy showed that the efficacy of a paraffin as a lubricant increases with increasing chain length. Also it is well known that the addition of a straight-chain acid increases the lubricating value of an unsubstituted paraffin. Probably several factors are at work here. For one thing, the acid molecules are more firmly anchored to the bearing surfaces; and again, as our experiment on the orientation of stearic acid molecules shows, they should reduce friction by orientating, and thus facilitating the leaning over of, the normal paraffin molecules, at the critical stage where, on reversal of the stroke in the engine cylinder, static friction gives way to conditions of dynamic friction.

The nature of bearing surfaces plays an important rôle in lubrication. The surface of a new bearing is relatively rough and has many minute peaks of soft crystalline material projecting above its mean level. For example, a mild steel surface brought to a fine finish with 0000 emery gives a good pattern of α-iron (Fig. 41), clear proof of the existence of sharp crystalline projections. A unimolecular oil film cannot effectively prevent metal-to-metal contact between such surfaces, for the load is borne by a few peaks and, since the oil film molecules are orientated with respect to the surface, the sharp contours of these peaks are precisely those places where the oil film is at its weakest. It is not until the process of polishing known as "running-in" under light loads has formed an amorphous Beilby layer that the oil can fulfil its proper functions of facilitating slip and preventing metal-to-

metal contact. Running-in is essentially a process of the melting by friction of the projecting peaks, whereby the valleys become filled with flowed material and the whole surface is smoothed and hardened by being converted into an amorphous condition. Between properly run-in surfaces the load is distributed over wide areas and there are no points of sharp curvature to weaken the oil film. Running-in produces an exceptionally deep Beilby layer and is thus a vigorous polishing process. Hopkins and Lees found that light polishing by hand produced a Beilby layer on copper or gold of less than 50 A. in thickness; in the case of a run-in internal combustion engine cylinder, however, the Beilby layer proved to be so thick that several light strokes with a fine emery paper were needed to break through to the crystal structure.

Cast-iron is a most interesting bearing metal. A cast-iron surface finished with fine emery might be expected to yield, like steel, a pattern characteristic of α-iron. Instead, it gives a pattern consisting of a series of parallel rows of practically equidistant diffuse spots, like Fig. 10, which is characteristic of graphite crystals orientated with their slip planes parallel to the cast-iron surface. In graphite the carbon atoms are tightly bound together into network sheets of hexagons, but the binding forces between the sheets are so slight that the layers can slip over each other like cards in a pack. Even when a cast-iron surface has been given the finest possible finish by careful running-in or polishing, the graphite pattern is distinctly to be seen superimposed on the haloes due to the iron Beilby layer (Fig. 42). The graphite is occluded in pores which open up on disturbance of the surface structure and distribute the graphite over the surface, where it is always ready to act as an emergency lubricant and to prevent metal-to-metal contact during any temporary breakdown of the oil film. Owing to its occluded graphite, cast-iron can be run in contact with a steel of similar melting point, or even with cast-iron, and give good service, though experience shows that it is otherwise bad practice to run together two metals of which the melting points do not differ widely.

An interesting experiment consists of the running-in together of a brass and a mild-steel surface. If, after running-in with a normal type of lubricating oil, the bearing is thoroughly freed from oil, a few minutes' further running results in seizure. On repeating the experiment, however, but with colloidal graphite added to the oil, the bearing can be run dry for a much longer period. Electron diffraction often fails to reveal the presence of graphite on such a bearing surface, but after slight etching, followed by gentle polishing to orientate any graphite crystals that may have been exposed, a graphite pattern is obtained, showing that during running-in with the graphited oil, minute graphite crystals have been, as it were, rolled into the Beilby layer during its formation, and in sufficient quantity to permit of prolonged dry running without seizure.

The shape of the graphite crystals in a colloidal solution is clearly revealed by electron diffraction. They consist of exceedingly thin flakes, each crystal containing on an average about ten sheets as is shown in patterns similar to Fig. 10 by the diffuseness of the diffractions corresponding to the spacings between the carbon layers. On the other hand, the sharpness of the diffraction phenomena (Fig. 43) due to atom rows lying in the hexagon planes shows that the average crystal extent in these directions must exceed 200 A. and may well be far greater. Indeed, many of the crystals are so large that they can be seen in the ultra-microscope and some even in the ordinary microscope. In shape, therefore, the average colloidal graphite crystal can be compared to a stack of a few large sheets of thin paper. Confirmatory evidence of the relatively large area and extraordinary thinness of these " sheets " is afforded by the fact that a transmission pattern like Fig. 43 contains certain extra diffractions (Fig. 44) which occur in directions not in accordance with Bragg's law, and from which it can be calculated that many particles have a thickness of only five or six atom layers.

It is interesting to note that an *X*-ray examination of colloidal graphite may give an entirely false impression of the crystal dimensions and shape, and may even suggest erroneously the existence of amorphous carbon, the absence of which is clearly testified to by the remarkable clarity and freedom from background in the electron-diffraction transmission patterns. Owing to high penetration, the strongest *X*-ray diffractions are those due to the spacings between the layers, and, as these are few, the diffractions are corre-

spondingly diffuse and form haloes resembling those obtained by either *X*-rays or electrons from amorphous carbon (Fig. 45). In the case of the very thin films formed by the evaporation of a drop of a dilute colloidal graphite solution on a thin celluloid film, however, the crystal sheets orientate parallel to the substrate. Thus the only diffractions obtained with the electron beam normal to the plane of such a specimen are due to atom rows in, or nearly in, the plane of the crystal flakes, and the diffraction phenomena are accordingly sharp and clear. A similar case is that of the exceedingly thin, sheet-like crystals of clays deposited from a colloidal solution or suspension (Fig. 46).

References.—References will be found in the following monographs: G. P. Thomson, "The Wave-mechanics of Free Electrons," McGraw-Hill, New York, 1930. F. Kirchner, "Elektronen- und Röntgen-Interferenzen," *Ergebn. exakt. Naturwiss.*, 1932, **11**, 64. J. J. Trillatt, "La Diffraction des Electrons et ses Applications," Act. Scient. et Industr., **269**, Hermann, Paris, 1935. G. I. Finch, A. G. Quarrell, and H. Wilman," Electron Diffraction and Surface Structure," *Trans. Faraday Soc.*, 1935, **31**, 1050. R. Beeching, "Electron Diffraction," Methuen, London, 1936. G. I. Finch and H. Wilman, "The Study of Surface Structure by Electron Diffraction," *Ergebn. exakt. Naturwiss.*, 1937, **16**, 353, contains a detailed discussion of the interpretation of the phenomena of the scattering and diffraction of electrons by films and surfaces, together with an extensive bibliography.

Imperial College, London, S.W.7.
Laboratoire de la Chaire Francqui, Brussels University.

Subtitles to the Illustrations (Figs. 1—46) to "Electron Diffraction and Surface Structure."

Fig. 1.—Halo pattern from polished copper.

Fig. 2.—Deposition of zinc on polished copper: (*a*) Diffraction pattern characteristic of crystalline zinc obtained immediately after deposition; (*b*) a few seconds later, the zinc pattern fades away owing to the dissolution of the zinc crystals in the copper polish layer. A zinc deposit on crystalline copper retains its characteristic crystalline structure.

Fig. 3.—Single-crystal type of pattern from a freshly cleaved surface of calcite.

Fig. 4.—The pattern from a highly polished cleavage surface is, like Fig. 3, typical of a single-crystal structure and shows that the polish layer is of single-crystal structure integral with the main body of the calcite crystal.

Fig. 5.—The polish layer on a calcite surface steeply inclined to all cleavage directions is amorphous and gives a halo pattern, but on heating it crystallises into a structure integral with the main crystal and then yields a typical single-crystal pattern.

Fig. 6.—Sodium nitrate crystals grown on a fresh or polished calcite cleavage surface are orientated in such a manner as to continue as closely as possible the structure of the calcite crystal.

Fig. 7.—Sodium nitrate does not orientate on the amorphous Beilby layer formed by polishing on a calcite surface steeply inclined to all cleavage directions.

Fig. 8.—Sodium nitrate orientates on the polish layer of Fig. 7 after it has been caused by heating to crystallise.

Fig. 9.—A polished diamond surface.

Fig. 10.—A polished graphite surface; the vertical row of diffractions is due to atom planes parallel to the cleavage directions.

Fig. 11.—The polish layer on a quartz single-crystal surface is crystalline and integral with the substrate structure.

Fig. 12.—A roughly polished spinel surface gives a pattern suggestive of crystal peaks integral with the main single crystal and projecting up into an amorphous Beilby layer. After completion of polishing, a halo pattern similar to Fig. 13 is obtained.

Fig. 13.—Halo pattern from a polished cassiterite crystal.

Fig. 14.—Transmission pattern through a polished aluminium oxide film. Normally the oxide is amorphous and gives only a halo pattern, but polishing has caused γ-Al_2O_3 crystals to form, and these give the sharp rings.

Fig. 15.—A thin aluminium single crystal heated in air gives a composite pattern of spots, due to the metal, rings due to γ-Al_2O_3 crystals formed by heating from the natural amorphous oxide layer which, in turn, gives rise to the faint haloes.

Fig. 16.—Single-crystal pattern obtained from a carborundum crystal which, prior to removal of the amorphous silica skin, only gave a halo pattern.

Fig. 17.—The same silicon carbide crystal gives a composite halo and single-crystal pattern after heating in a Bunsen flame; a film of amorphous silica is formed, but it is so thin that some electrons can traverse the film to be scattered by the silicon carbide crystal and emerge again without energy loss.

Fig. 18.—A unimolecular n-$C_{22}H_{46}$ layer on a quartz surface gives a typical "layer-line" pattern, but is not thick enough to obscure the pattern due to the quartz crystal.

Fig. 19.—A n-$C_{32}H_{66}$ monolayer on quartz gives a pattern characteristic of the hydrocarbon alone. Thus the upper limit of penetration of the electron beam at grazing incidence must be less than 43 A.

Fig. 20.—α-Ferric oxide (rhombohedral structure) formed by heating iron in air; the ring definition shows that the crystals are relatively large.

Fig. 21.—γ-Ferric oxide or ferrosoferric oxide (cubic) formed by "blueing" iron in steam.

FIG. 1.

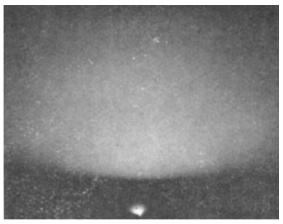

FIG. 2.

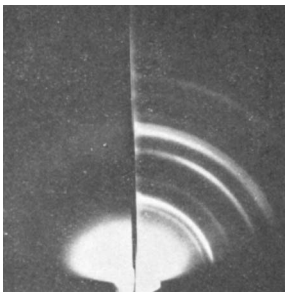

FIG. 5.

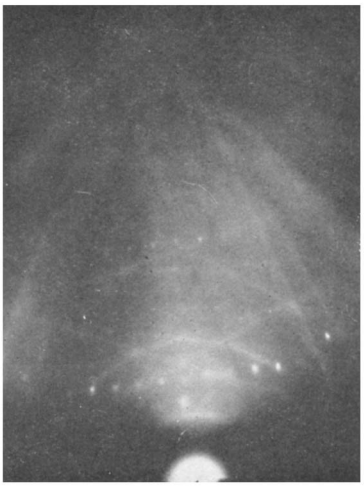

FIG. 3.

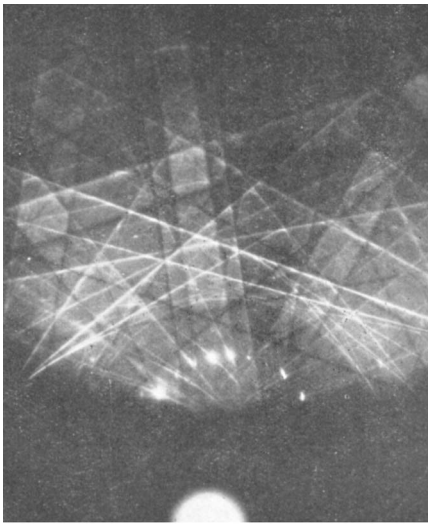

FIG. 4.

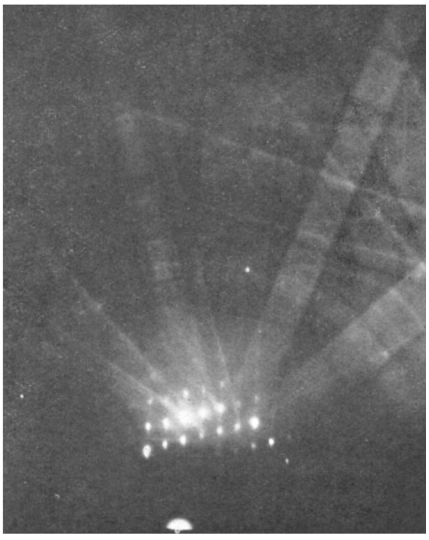

FIG. 6.

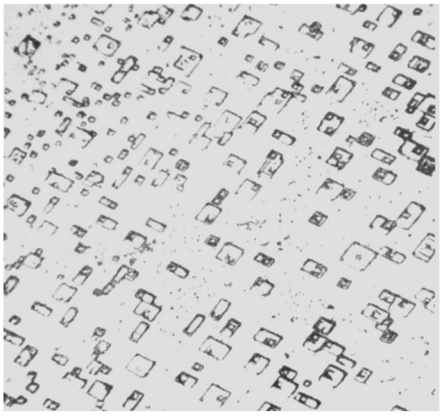

FIG. 7.

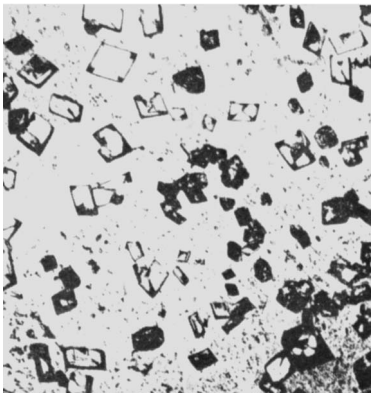

[*To face p.* 1146.

FIG. 8.

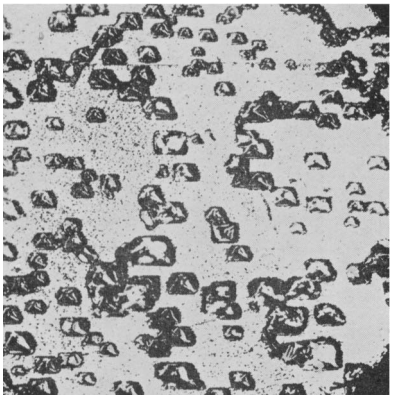

FIG. 9.

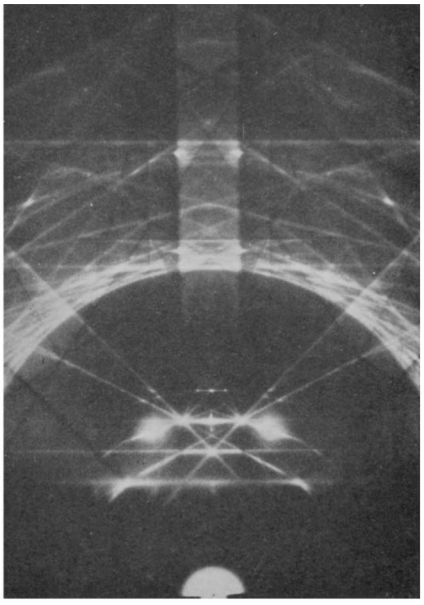

FIG. 10.

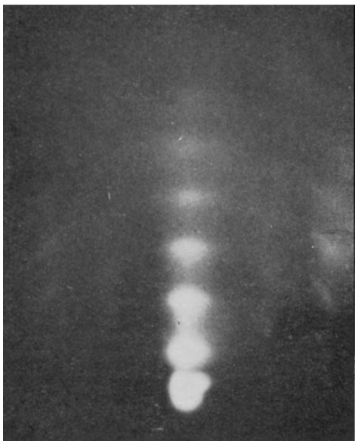

FIG. 11.

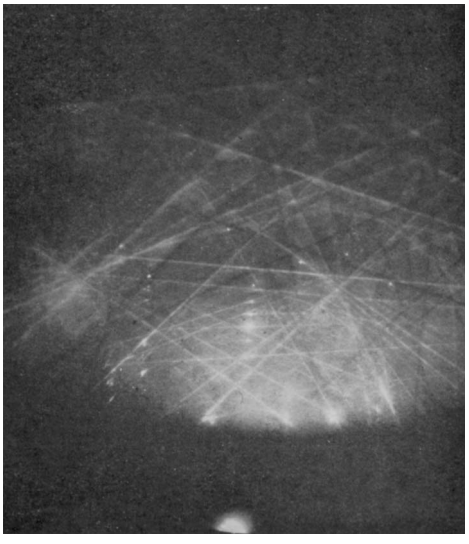

FIG. 14.

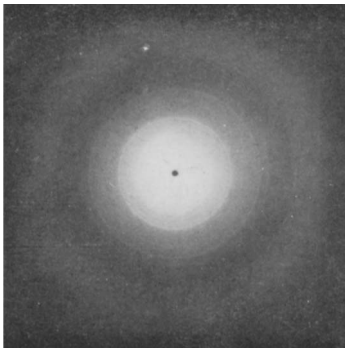

FIG. 12.

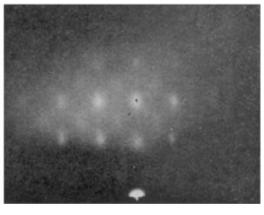

FIG. 13.

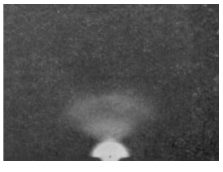

FIG. 15.

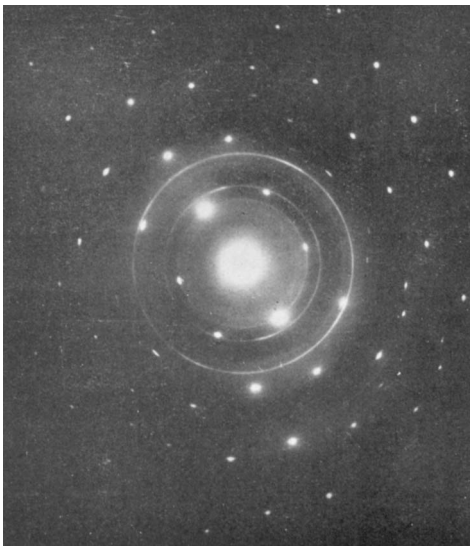

FIG. 16.

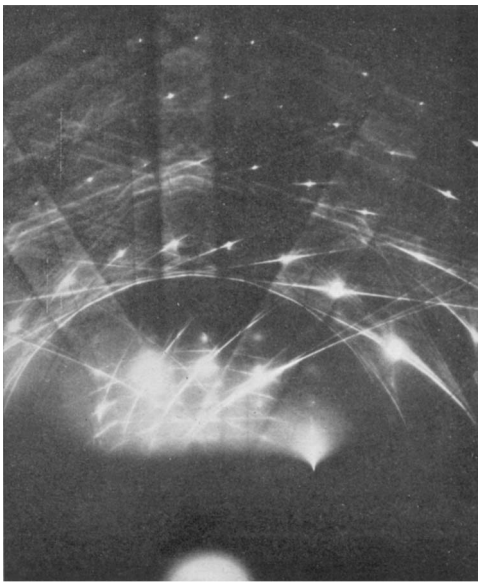

FIG. 18.

FIG. 17.

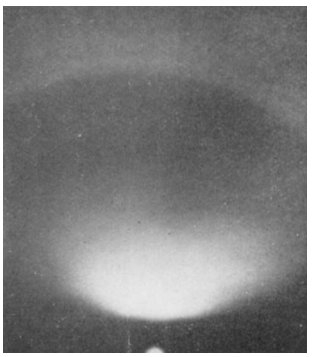

FIG. 19.

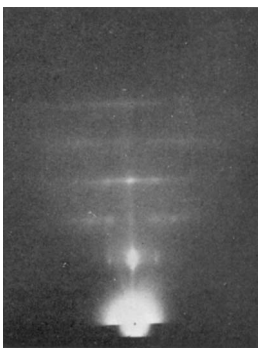

FIG. 21.

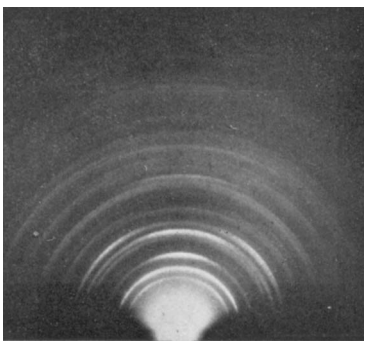

FIG. 20.

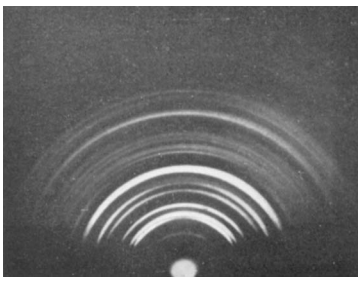

FIG. 22.

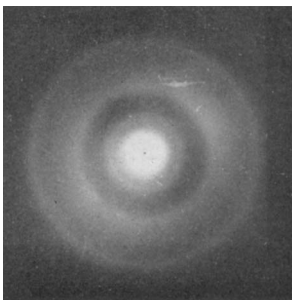

FIG. 23.

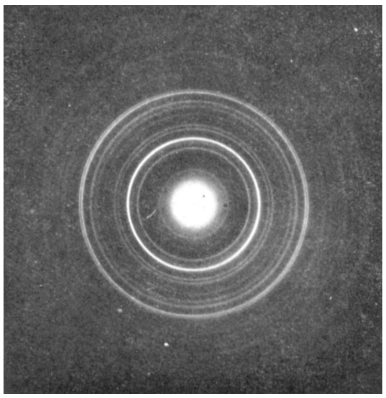

FIG. 25.

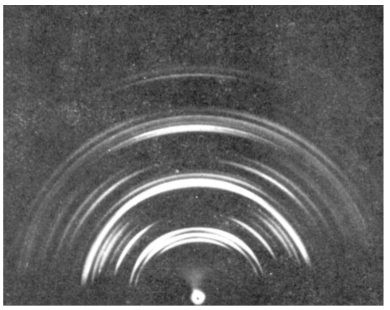

FIG. 24.

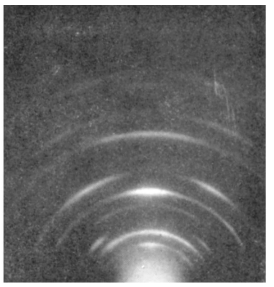

FIG. 26.

FIG. 27.

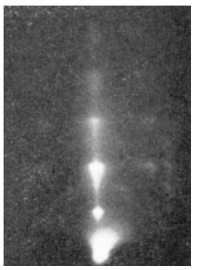

FIG. 29.

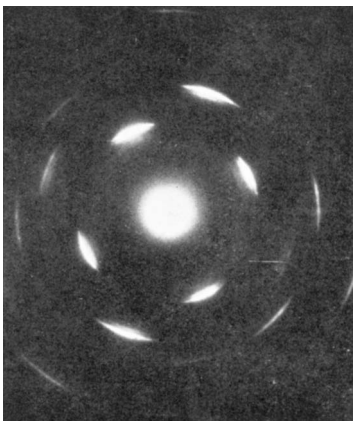

FIG. 28.

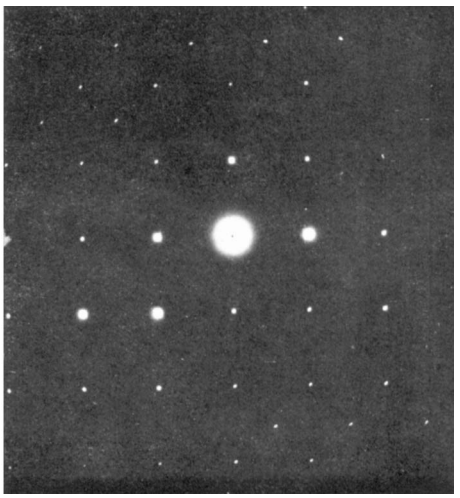

FIG. 30.

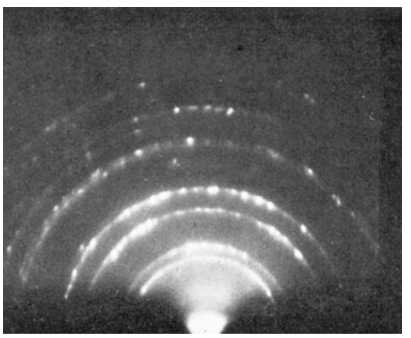

FIGS. 32 and 33.

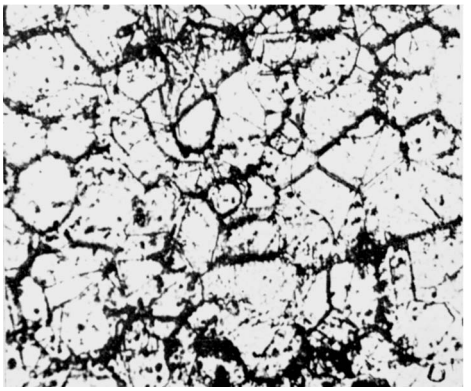

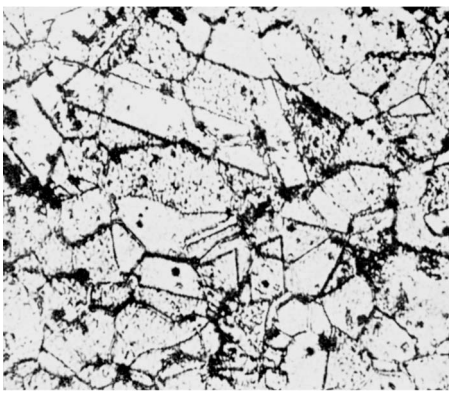

FIG. 31.

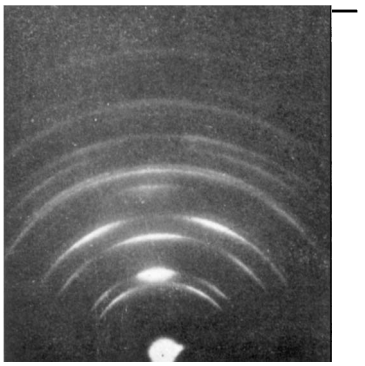

FIG. 34.

FIG. 35.

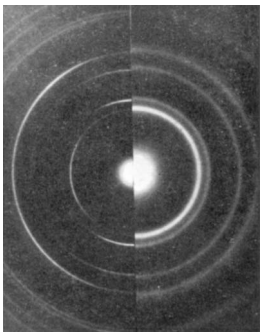

FIGS. 36 and 37.

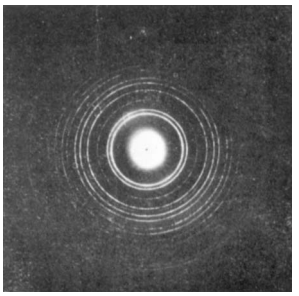

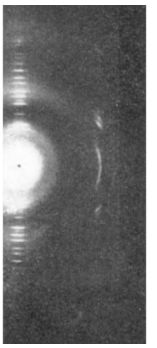

FIG. 38.

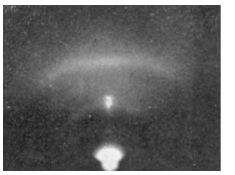

FIG. 39.

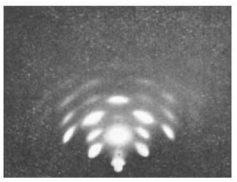

FIG. 40.

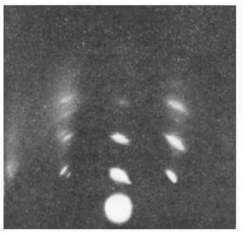

FIG. 41.

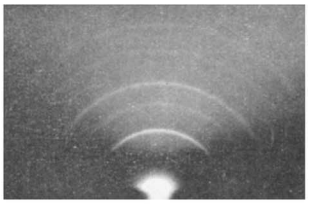

FIG. 42.

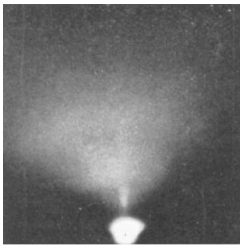

FIG. 46.

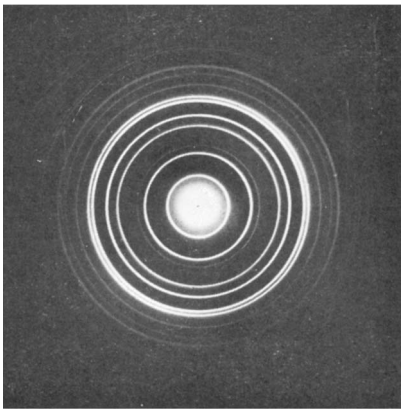

FIG. 44.

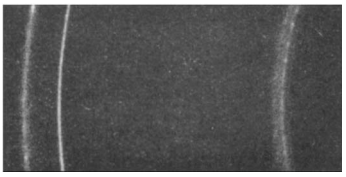

FIG. 45.

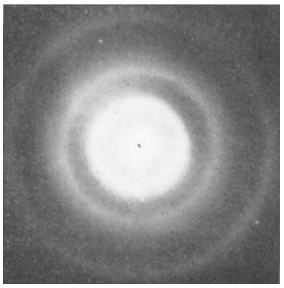

FIG. 43.

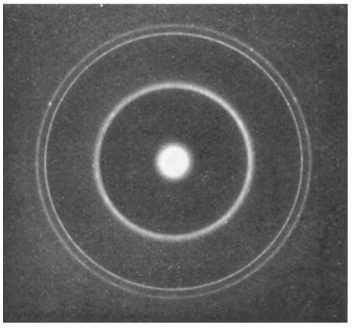

FIG. 22.—Amorphous oxide film formed by passivation of iron in nitric acid.
FIG. 23.—On heating, the amorphous iron oxide crystallises and is no longer protective; the structure is as in Fig. 21.
FIG. 24.—Cuprous oxide (cubic).
FIG. 25.—Cupric oxide (monoclinic).
FIG. 26.—Nickel selenide, $NiSe_2$ (has the same structure as FeS_2).
FIG. 27.—Mercuric bromide crystals (rhombic) formed on mercury are orientated with the (010) plane parallel to the surface of the liquid.
FIG. 28.—Ag single crystal grown by deposition of vapour on a heated rocksalt cleavage surface. The pattern was taken with the electron beam parallel to a cube edge.
FIG. 29.—Iron crystals formed by electrodeposition on gold orientate so that cube faces are in contact but the respective crystals are rotated to each other by 45° in the plane of contact.
FIG. 30.—In a thin layer of nickel on macrocrystalline copper the crystal size and orientation follow that of the substrate.
FIG. 31.—When the layer is thicker, the crystal size and orientation of the nickel deposit is no longer determined by the substrate, but is characteristic of the deposition conditions.
FIGS. 32 and 33.—Microphotographs of the surfaces of Figs. 30 (thin Ni deposit) and 31 (thick Ni deposit) reveal no change.
FIG. 34.—Aluminium crystals grown on platinum and which have basal dimensions similar to those of Pt but normal spacings in the other dimension.
FIG. 35.—A comparison shutter record of a Pt–Ag alloy formed by chemical displacement (right) with gold as standard (left).
FIGS. 36 and 37.—Transmission patterns through a thin film of $C_{32}H_{66}$ supported on celluloid and taken with the beam normal and steeply inclined respectively to the film.
FIG. 38.—Stearic acid.
FIG. 39.—Polished stearic acid surface; the beam is along the direction of rubbing and the pattern is symmetrical about the vertical through the undeflected beam spot.
FIG. 40.—Asymmetric pattern obtained from the surface of Fig. 39 with the beam normal to the direction of rubbing.
FIG. 41.—α-Iron crystals on abraded mild steel.
FIG. 42.—Pattern from a run-in cast-iron cylinder. The halo pattern due to the Beilby layer is superimposed on the diffuse spot pattern of orientated graphite crystals.
FIG. 43.—Transmission through a film of orientated colloidal graphite flakes. The 110 ring, for example, is very sharp; also, its distinctly granular appearance testifies to the presence of crystals of microscopic dimensions in the cleavage plane directions.
FIG. 44.—An enlarged section of Fig. 43. The innermost broad band is resolved into four rings; two of these only appear because the flakes are extremely thin (about 30 A.).
FIG. 45.—Halo pattern from benzene soot.
FIG. 46.—Transmission pattern from bentonite crystals orientated with the (001) planes normal to the electron beam.